Modeling and Investigation of Dynamic Recrystallisation in Nickel-Based Superalloys

C. Sommitsch[1], M.Walter[2], F. Wedl[3] and S. Kleber[4]

[1-4] Böhler Edelstahl GmbH & Co KG, P.O.Box 96, A-8605 Kapfenberg, Austria,
christof.sommitsch@bohler-edelstahl.at

Abstract. A process model for the calculation of the microstructure evolution of nickel-based alloys during a hot forming process helps to optimise the forming process and to achieve the desired microstructure. In the grain structure model, the mean dislocation density rate within a homogeneous area can be estimated by the summation of a work hardening and a recovery rate. If a critical dislocation density is reached, recrystallisation nuclei will form. This critical dislocation density and the correspondent critical nucleus size can be calculated with a nucleation criterion for dynamic recrystallisation. During dynamic recrystallisation the nucleation process takes place at the grain boundaries of the deformed grains. The number of grains as a function of time is described by both a phenomenological and a physical based approach. The model was tested by a comprehensive experimental programme with the Alloy 80A.

Introduction

Microstructure simulations typically address three salient points: first, they aim at improving our insight into the underlying physical principles that govern the nature of microstructure evolution at the various scales. This task falls into the domain of elaborating physically plausible structural evolution laws. Second, they provide quantitative microstructure-property relations. This point can be regarded as a contribution to identifying appropriate microstructure equations of state. Third, they allow us to investigate both of the aforementioned aspects at levels that are not amenable to experimentation or under conditions that have not yet been studied. The latter aspect is particularly important for introducing simulations in industry [1].

Finite Element and *Difference Methods* and also *Polycrystal Elasticity* and *Plasticity Models* represent the modeling approach at the mesoscopic-macroscopic scale to which the presented model [2,3] belongs to. It can be classified as an advanced microstructure finite element model (microstructure mechanics). It simulates the grain structure development during and after hot deformation of nickel-base alloys and considers normal grain growth, dynamic, meta-dynamic and static recrystallisation and can be used for alloys with low stacking fault energies and thus recrystallisation as the predominant softening mechanism. In this paper the main emphasis is given on the aspects of the nucleation and growth of dynamically recrystallised grains.

For the model validation a comprehensive experimental program on a Gleeble 3800 testing system has been conducted (this work and [4]).

Nucleation Models

Criteria for Dynamic Recrystallisation. During hot forming, the derivative of the dislocation density can be described [5] by the equation

$$\frac{d\rho}{dt} = \frac{\dot{\varepsilon}}{b\,l} - 2\,M\,\tau\,\rho^2, \qquad (1)$$

taking the strain hardening and the recovery of dislocations into account, where $\dot{\varepsilon}$ is the strain rate, b the Burgers vector, l the mean free path of the dislocations, M the mobility of recovery and τ the average energy per unit length of a dislocation.

A critical dislocation density is necessary in order to initiate dynamic recrystallisation. The nucleus usually forms at pre-existing grain boundaries in the material, at least at higher strain rates. For an area that has just been recrystallised it is assumed that the dislocation density ρ_0 generated by the preceding strain is reduced to a very low value. Roberts and Ahlblom [6] developed a nucleation criterion, which is based upon the idea that during dynamic recrystallisation, the concurrent deformation reduces the stored energy difference (driving force) that effects migration of a high angle boundary. The nucleation theory gives the net free energy change [6]

$$\Delta G(r) = -\frac{4}{3}\pi r^3 \frac{\tau}{r}\int_0^r [\rho_0 - \rho(x)]dx + 4\pi r^2 \gamma_{GB} \qquad (2)$$

where γ_{GB} is the grain boundary energy per unit area, $\rho(x)$ the increasing dislocation density behind the boundary and r the radius of a spherical nucleus.
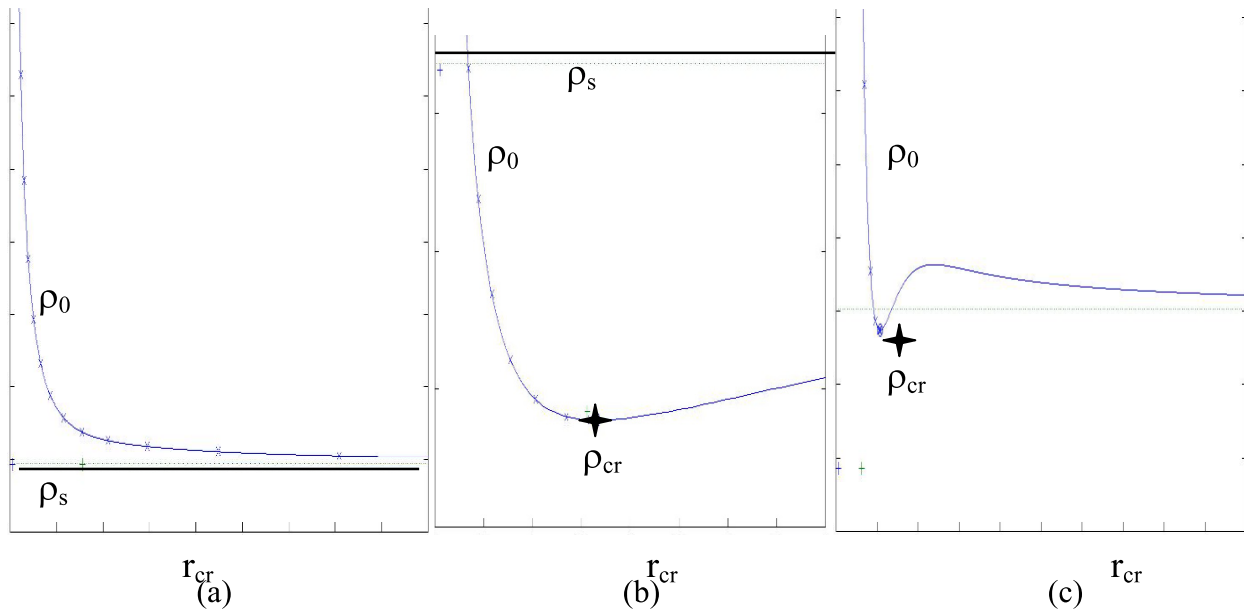

Fig. 1: Determination of the critical radius of a recrystallisation nucleus and the corresponding critical dislocation density for the onset of dynamic recrystallisation. The critical dislocation density is found at the minimum of ρ_0 (a,b). If the local conditions are so that ρ_0 does not fall short of the stationary dislocation density ρ_s, no dynamic recrystallisation will be initiated (c).

Maximising the net free energy change produces the critical nucleation conditions:

$$r_{cr}\tau\left[\frac{\rho_s}{3}\tanh\left(2\frac{M}{m}\frac{\rho_s}{\rho_0}r_{cr}\right) - \rho_0\right] + \left(\frac{\tau\rho_0 m}{3M}\right)\ln\left[\cosh\left(2\frac{M}{m}\frac{\rho_s}{\rho_0}r_{cr}\right)\right] + 2\gamma_{GB} = 0, \qquad (3)$$

where m denotes the mobility of a moving high angle boundary and ρ_s the stationary dislocation density [6]. No real critical radius r_{cr} exists unless ρ_0 exceeds a critical value ρ_{cr}. Substituting ρ in eq. (1) with ρ_{cr} will give the critical time t_{cr} for a given strain rate.

Fig. 1 shows schematically three types of results that correspond to eq. 3 and which depend on different local deformation conditions.

Phenomenological Model. The nucleation with time can be described phenomenologically by the number of nuclei per volume as a function of time $Z(t)$

$$Z(t) = Z_\infty \left(1 - \exp(-\alpha\, t)\right),$$

(4)

where Z_∞ denotes the asymptotic number of nuclei per volume for $t \rightarrow \infty$ and α is an exponential variable. It results from preliminary calculations that α has to be in proportion to the gradient of the dislocation energy $\tau\rho/d_{gb}$:

$$\alpha = \frac{m\,\tau\,\rho_{cr}}{d_{gb}} K_\alpha,$$

(5)

where d_{gb} is the 'thickness' of the grain boundary and K_α is a constant factor. Further reading of this approach can be found elsewhere [2,3].

Physically Based Model. Dynamic recrystallisation can be considered in terms of the rate of nucleation (formation of interfaces) versus the rate of growth (migration of interfaces) under given boundary conditions. A model that considers the dynamic balance of these two rates was proposed by Srinivasan and Prasad [7]. The nucleation consists of the formation of a grain boundary due to dislocation generation, and simultaneous recovery and rearrangement. This interface will become a nucleus for dynamic recrystallisation when it attains a critical configuration, i.e. that of a high angle boundary. The nucleus will grow by the process of grain boundary migration. Since under hot working conditions the material acts essentially as a dissipator of power, the driving force for the migration of interfaces is the reduction of total interface energy. When nucleation and growth occur simultaneously, the slower of the two will control dynamic recrystallisation.

The rate of annihilation of recovered groups of dislocations (interfaces) as a result of migration of interfaces depends upon the mobility of the boundary. On the other hand, the rate of interface formation depends on the rate of generation of recovered dislocations. In [7] it is shown that for nickel the rate of nucleation is lower than the rate of growth by about four orders of magnitude and therefore controls the dynamic recrystallisation process. For nickel and nickel-based superalloys with their relatively low stacking fault energies at high temperatures, mechanical recovery involving cross slip of screw dislocations can be neglected in comparison with thermal recovery based on climb of edge dislocations. Hence the rate of interface formation R_F for these types of alloys can be described by

$$R_F = \frac{\dot{\varepsilon}\, P_R}{b\, l} = K_F\, l\, v_c\, \rho_{cr}^2,$$

(6)

where P_R is the probability of recovery of dislocations, K_F is a constant and v_c is the climb velocity of edge dislocations.

Let us assume that nuclei form at the boundaries of the deformed grains with diameter d_0. Hence the number of nuclei Z can be calculated by

$$Z(t) = \int J_F\, dt = \int \frac{R_F}{N_d\, d_0}\, dt,$$

(7)

where J_F is the nucleation rate per volume, $N_d = A_{cr}/l_{cr}^2$ is the number of dislocations per critical nucleus, A_{cr} is the cross section of a critical nucleus and l_{cr} is the mean free path of dislocations with a critical density ($l_{cr} \sim \rho_{cr}^{-1/2}$).

Recrystallisation Model

The following model is described in detail in [2,3]. The recrystallised fraction $f(t_b)$ at the time t_b is given by the sum over all nucleation times t_g:

$$f(t_b) = \frac{\pi}{6} \int_{t_{cr}}^{t_b} D^3(t_g, t_b) Z'(t_g) dt_g \ , \qquad (8)$$

where $D(t_g, t_b)$ is the size of a grain class, nucleated at the time t_g and $Z'(t_g) \, dt_g$ grains are nucleated in the time interval $[t_g, t_g + dt_g]$. It must be considered that the growing grains touch with time. Therefore only a fraction of the boundary will move [3].
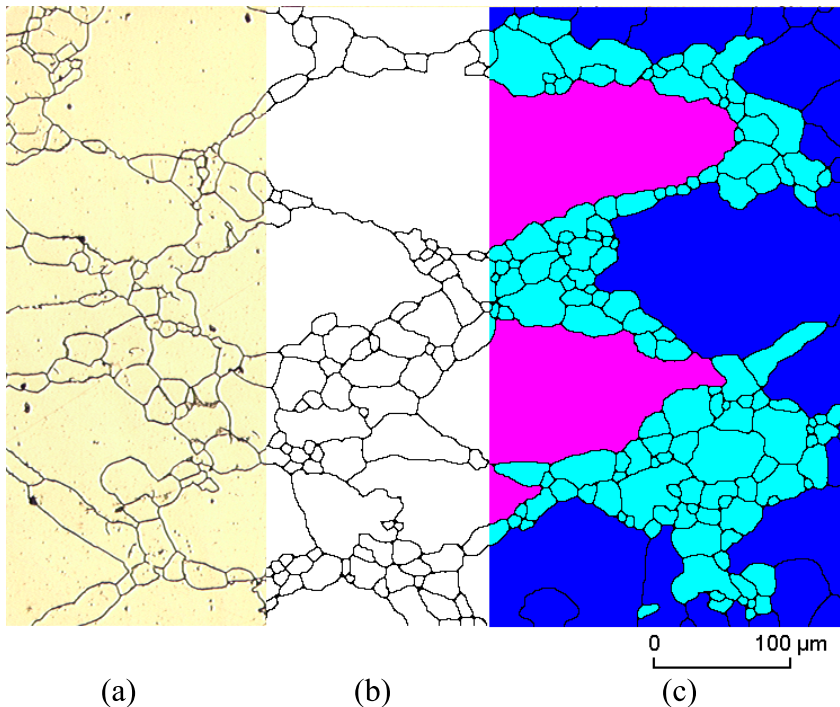
Experimental Program

Fig. 2: Partially recrystallised microstructure: Etched (a), binary (b) and analysed (c) section.

Gleeble Tests. Experiments were performed to confirm the simulation of dynamic recrystallisation on measured recrystallised fraction, nucleus density and grain size distribution data. Samples of Böhler L306 VMR (Alloy 80A) were cut from hot rolled pieces, thus ensuring a completely recrystallised, fine-grained and homogeneous microstructure. Hot compression tests were carried out on a Gleeble 3800 testing system. Solution heat treatment was done at 1220°C for 60 seconds. The short annealing time was chosen to avoid grain growth. This lead to an initial grain size of 120µm. The specimens were cooled down to the test temperature of 1120°C and were compressed at a constant strain rate of 0.1/s to strains of 0.05, 0.10,…,0.95,1. The cylindrical compression samples (h=12mm, d=10mm) were cut to both longitudinal (specimen center) and transversal cross sections. The latter sections were chosen at a quarter of the specimen height. Finite element calculations of the compression tests proved that in this section from the center to half the radius,

the local and the global strain rate correspond. The investigations of the microstructure were done both by an image analysis system and electron diffraction.

ImageC. The grinded and polished transversal and longitudinal sections were electrolytically etched. One quarter of every longitudinal and transversal section was evaluated with the commercial imaging system ImageC$^{©}$. The first step in analysis is the transformation of the multi colour image to a binary black and white image with closed grain boundaries. Several standard tools of the imaging software were combined in a self-made macro program to reach an optimum and reproducible transformation (fig. 2a,b). Afterwards a standard analysing tool of the software is able to detect and calculate the area [μm^2] and the chord length [μm] under 0°, 45°, 90° and 135° of every single grain. All grains overlapping with the image frame were excepted from the evaluation. To distinguish between recrystallised and deformed grains a critical size has to be fixed arbitrarily (fig. 2c).

EBSD. In the following the investigations are focused on the transversal cross sections of the specimens. The investigations were performed by the *Center for Electron Microscopy Graz*, Austria. The samples were polished using colloidal silica. The analysis of the samples took place using a *Leo Gemini 938*. The EBSD software *OIM-TSL-Analysis 3* was used for the collection of orientation data. With the orientation imaging system, grains are separated due to their orientation difference (high angle grain boundary). The minimum orientation difference of two points of adjacent grains was fixed at 5°. Only grains with a minimum of 6 measuring points were considered which lead to a minimum grain size of 6μm. Recrystallised and deformed grains were distinguished by the orientation spread within a grain (fig. 3a). The area fractions of recrystallised and deformed grains were analysed in terms of grain size distributions, recrystallised fractions and densities of overcritical recrystallisation nuclei (fig. 3b).
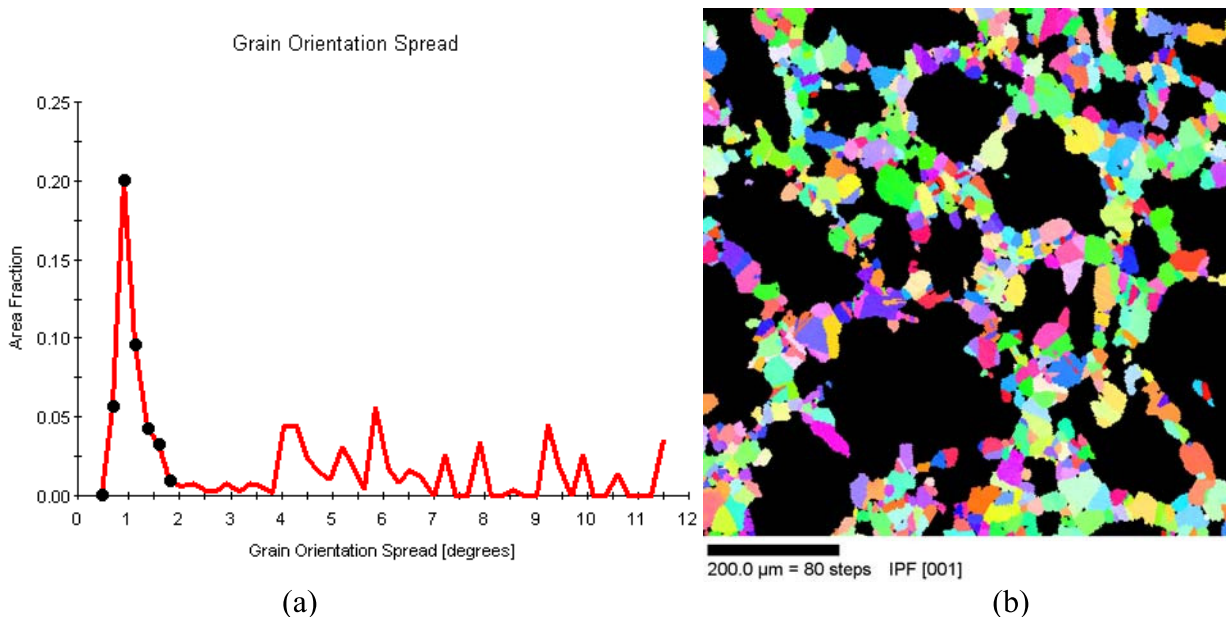

(a) (b)

Fig. 3: Sample at a local strain of 0.5. Recrystallised fraction: 44%. Orientation spread distribution of grains: The maximal grain orientation spread of recrystallised grains was set to 2° (a). Deformed grains (black) and recrystallised grains: necklace structure (b).

Conclusions

Nucleus Density. In fig. 4a it is shown that both models are able to describe the ongoing nucleation. With the phenomenological nucleation model, the moving boundary fraction decreases with recrystallisation after the impingement of recrystallised grains. This fact is not yet incorporated into the physical model, hence the nucleation rate does not decrease with time. The

differences of the EBSD and the ImageC results are based on the fact that the imaging system can not relate the deformed grains which are smaller than the critical grain size to the unrecrystallised fraction. In a metallographical section there is always a certain amount of grains cut near the corners.

Recrystallised Fraction. Due to the latter described misinterpretation of small deformed grains in the imaging system, the ImageC results are quite higher than those from the EBSD method. To consider this mismatch which decreases with increasing recrystallised fraction, the fraction obtained by ImageC was modified by $f_{mod} = f^2$. It is evident from fig. 4b that the imaging analysis system can only deliver physically meaningful results up to 60-70%. This follows from the fact that at this stage of recrystallisation both the recrystallised and deformed grains approximate in their size. Hence an arbitrarily chosen critical grain size as a distinction criterion can only be used up to this percentage and with the prerequisite that the recrystallisation nuclei are quite smaller than the deformed grains. This assumption should be usually valid for dynamic recristallisation, but not conclusive for static recrystallisation.
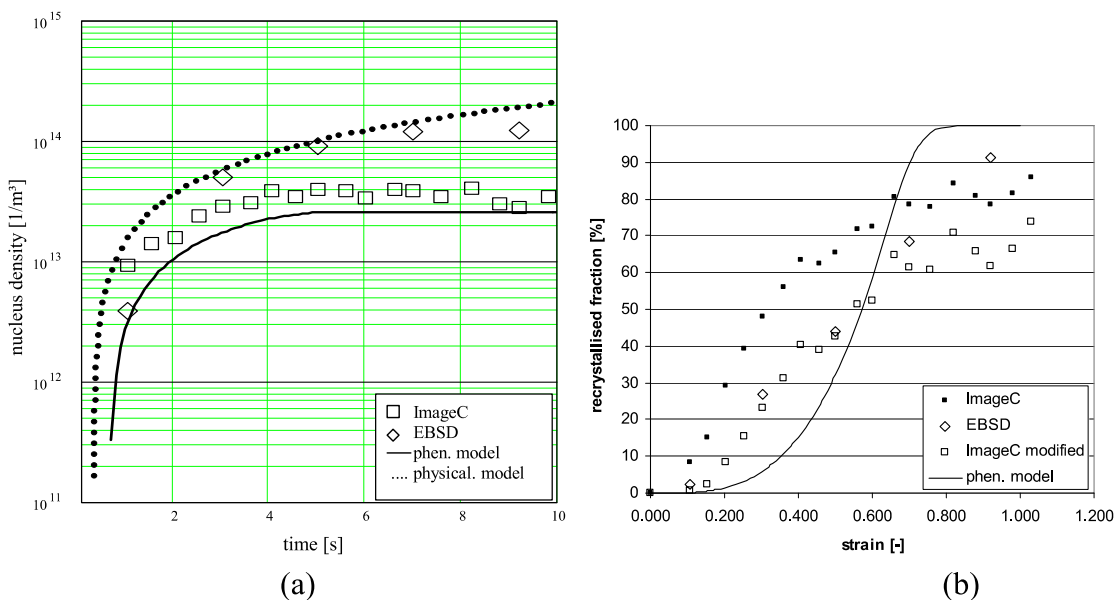

(a)   (b)

Fig. 4: Comparison of the nucleus density (a) and the recrystallised fraction (b) between experiments and calculations.

References

[1] D. Raabe: *Computational Materials Science* (D. Raabe (Ed.), Wiley-VCH, Weinheim, Germany 1998, p. 303).

[2] C. Sommitsch: *Ph.D. Thesis*, Institute for Materials Science, Welding and Forming, Graz University of Technology, Graz, Austria 1999.

[3] C. Sommitsch, V. Wieser and S. Kleber: J. Mat. Proc. Vol. 125-126 (2002), p. 130.

[4] G. Bock: *Diploma Thesis*, Institute for Materials Science, Welding and Forming, Graz University of Technology, Graz, Austria 1998.

[5] R. Sandstroem and R. Lagneborg: Acta Met. Vol. 23 (1975), p. 387.

[6] W. Roberts and B. Ahlblom, Acta Met. Vol. 26 (1978), p. 801.

[7] N. Srinivasan and Y.V.R.K. Prasad, Mat. Sci. Techn. Vol. 8 (1992), p. 206.